2014 International Joint Conference on Neural Networks (IJCNN)
July 6-11, 2014, Beijing, China

Clustering and Synchronous Firing of Coupled Rulkov Maps with STDP for Modeling Epilepsy

Naohiro Shibuya[1], Charles Unsworth[2], Yoko Uwate[1] and Yoshifumi Nishio[1]

***Abstract*— Epilepsy of the neuropsychiatric disorder is provoked from an imbalance in the long-term potentiation (LTP) versus long-term depression (LTD) of the synapses in the hippocampus. The LTP and LTD are replicated by using the Spike Timing Dependent Plasticity (STDP). Additionally, the spiking activity of the synapses in the hippocampus can be approximated by using the Rulkov maps. In our previous study, we considered some easy simulation models which are constructed by using Rulkov maps with STDP. Moreover, these simulation models consist of unidirectionally coupled neurons. In this paper, we consider some easy simulation models with bidirectionally coupled neurons. We explore the effect of unidirectional and bidirectional connection on spiking activity, as basic simulation for constructing the approximate simulation model of epilepsy. From these results, the unidirectional models show high accuracy in-phase/anti-phase synchronization, and it shows divergent relatively early. The bidirectional models show the stable waveform (i.e., non-divergent) for a long term compared to unidirectional models.**

I. Introduction

EPILEPSY is known as one of neuropsychiatric disorder and involved with a large part of the hippocampus. The hippocampus has the lowest seizure threshold in the brain, therefore it has indicated the beginning of most epilepsy seizures. Moreover, the seizure-related neuronal electrical activity has feature of synchrony arising regularly [1]. In the normal status, some neurons suppress the abnormal firing. If the neuronal firing property of neurons or potentiation and depression balance are altered slightly, the supranormal excitability is diffused and lead to seizure. We consider that the each potentiation and the depression corresponds approximately to each long-term potentiation (LTP) and long-term depression (LTD).

In this study, we apply Spike Timing Dependent Plasticity (STDP) to Rulkov maps for constructing the small-scale simulation models. STDP is a generic model used to replicate the LTP and the LTD [2], and Rulkov Map produces two-dimensional spiking-bursting behavior like real biological neurons [3],[4]. By incorporating the STDP into the original Rulkov Map, we can explore the synchronous behavior like real biological spiking activity. We investigate a relationship between synchronous firing and LTP, LTD. Moreover, we explore the effect of unidirectional and bidirectional connection on spiking activity, as basic simulation for constructing the approximate simulation model of epilepsy.

Naohiro Shibuya[1], Yoko Uwate[1] and Yoshifumi Nishio[1] are with the Department of Electrical and Electric Engineering, University of Tokushima, Tokushima, Japan (email: {shibuya, uwate, nishio}@ee.tokushima-u.ac.jp).

Charles Unsworth[2] is with the Department of Engineering Science, The University of Auckland, Auckland, New Zealand (email: c.unsworth@auckland.ac.nz).

II. Spike Timing Dependent Plasticity

STDP is a temporally asymmetric form of Hebbian learning induced by tight temporal correlations between the spikes of pre-synaptic and post-synaptic neurons. STDP provokes the LTP of the synapses, if the pre-synaptic spike arrival a few milliseconds before post-synaptic spikes. Whereas, it provokes the LTD of the same synapse, if pre-synaptic spike arrival after post-synaptic spikes.

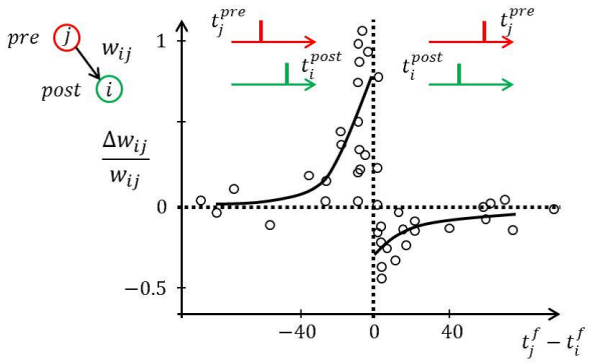

Fig. 1. The STDP function of changing synaptic connection.

The weight change Δw_{ij} depends on the relative timing between pre-synaptic spike arrivals and post-synaptic spikes. The total weight change Δw_{ij} induced by a simulation protocol with pairs of pre-synaptic and post-synaptic spikes is described as following.

$$\Delta w_{ij} = \sum_{f=1}^{N} W(t_j^f - t_i^f) \tag{1}$$

where $W(x)$ denotes one of the STDP functions in Fig. 1. The method to choose for the STDP function $W(x)$ is shown as following.

$$W(x) = \begin{cases} A_+ exp(-x/\tau_+) & (x < 0) \\ -A_- exp(x/\tau_-) & (x > 0) \end{cases} \tag{2}$$

which has been used in fits to experimental data and models. The parameters A_+ and A_- may depend on the current value of the synaptic weight w_{ij}. In this article, the parameter A_+ and A_- are fixed 0.05 each, and the time constants are on the order of $\tau_+ = [10ms]$ and $\tau_- = [10ms]$.

978-1-4799-1484-5/14/$31.00 ©2014 IEEE

III. Coupled Rulkov Maps

In recent years, a simple model which replicates the dynamics of spiking and spiking-bursting activity of real biological neurons has proposed by N. F. Rulkov. The model is a two-dimensional map that produces chaotic spiking-bursting neural behavior. It is demonstrated that the results of this model are in agreement with the synchronization of chaotic spiking-bursting behavior experimentally found in real biological neurons. The expressions of the coupled Rulkov maps are shown as following.

$$\begin{aligned} x_{m,n+1} &= f(x_{m,n}, x_{m,n-1}, y_{m,n}) \\ &\quad + \frac{1}{2} w_{ij}(x_{m+1,n} - 2x_{m,n} + x_{m-1,n}) \\ y_{m,n+1} &= y_{m,n} - \mu(x_{m,n} + 1) + \mu\sigma + \mu\sigma_{m,n} \\ &\quad + \frac{1}{2} w_{ij}(x_{m+1,n} - 2x_{m,n} + x_{m-1,n}) \end{aligned} \tag{3}$$

where x is the fast and y is the slow dynamical variables and the parameter w_{ij} shows the coupling weight of the connection between the map. The coupling weights w_{ij} are updated by STDP function. If STDP provokes the LTP, the coupling weights are updated to positive direction. Whereas, if it provokes LTD, the coupling weights are updated to negative direction. The nonlinear function $f(x_n, x_{n-1}, y_n)$ is shown as following:

$$f(x_{m,n}, x_{m,n-1}, y_{m,n}) = \begin{cases} \alpha/(1 - x_{m,n} + y_{m,n}), & (x_{m,n} \leq 0) \\ \alpha + y_{m,n}, & (0 < x_{m,n} < \alpha + y_{m,n} \ and \ x_{m,n-1} \leq 0) \\ -1, & (x_{m,n} \geq \alpha + y_{m,n} \ or \ x_{m,n-1} > 0) \end{cases} \tag{4}$$

α, σ and μ show the parameters of the maps. In this paper, we set parameter α, σ and μ with arbitrary value. Here, these parameters are the control parameters of the dynamics, and each activity shows the typical behavior of the neurons. Specifically, the amplitude of waveform is changing by parameter α.

IV. Network Models and Simulations

In this section, we consider some easy simulation models to analyze CA3 hippocampus network model, and observe the synchronous firing phenomena of coupled Rulkov maps.

A. CA3 Hippocampus Network Model

The network model of CA3 hippocampus is shown in Fig. 2. CA3 hippocampus network consists of pyramidal cells (excitability) and intercalated cells (inhibitory). The pyramidal cells are interconnected with 8 pyramidal cells of neighborhood. Moreover, the intercalated cells are interconnected with 16 pyramidal cells of neighborhood.

Additionally, the pyramidal cells and the intercalated cells exhibit spiking/bursting activity as shown in Fig 3. We set the parameter of Rulkov maps for replicating the spiking/bursting activity of the pyramidal cells and intercalated

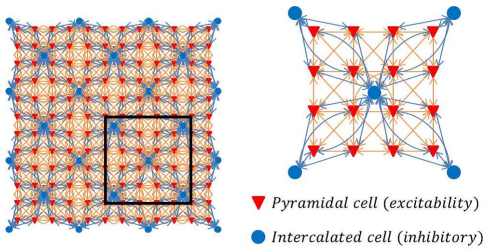

Fig. 2. Network structure of CA3 hippocampus.

cells. The parameter α, σ and μ are set to 50, 0.1 and 0.04 ~ 0.06 each for the pyramidal cells. Moreover, the parameter α, σ and μ are set to 40, 0.33 and 0.6 each for the intercalated cells.

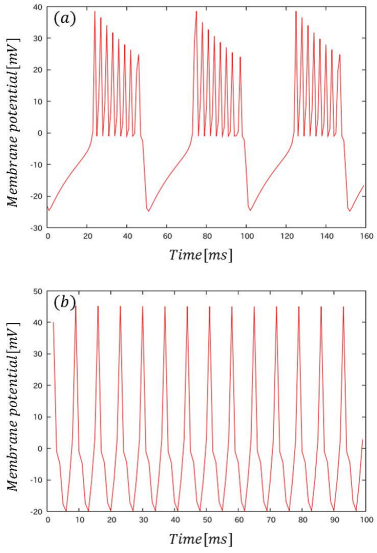

Fig. 3. Spiking activity. (a) Pyramidal cells. α = 50, σ = 0.1, μ = 0.05. (b) Intercalated cells. α = 40, σ = 0.33, μ = 0.6.

B. 2 Coupled Maps of unidirectional model

In this section, we observe fundamental synchronization phenomena of the 2 coupled Rulkov maps of unidirectional models as shown in Fig. 4.

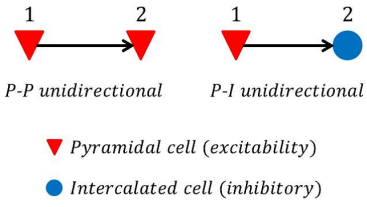

Fig. 4. Connective arrangements of 2 coupled maps in unidirectional model.

Moreover, we define the synchronization probability to provide quantitative analysis of synchronization accuracy. The synchronization probability is defined as follows.

$$I = \frac{Y}{X} \tag{5}$$

where X is the number of burst waveform, and Y is the number of synchrony burst waveform. The coupled Rulkov maps shows in-phase synchronization, if the synchronization probability closes in the value to 1. Whereas, it shows anti-phase synchronization, if the synchronization probability closes in the value to 0.

The spiking activity and the coupling weight of P-P unidirectional model are shown in Fig. 4, and Table 1 shows the synchronization probability of P-P unidirectional model if the parameter μ of coupled Rulkov maps is set to 0.04, 0.05 and 0.06.

TABLE I
SYNCHRONIZATION PROBABILITY OF P-P UNIDIRECTIONAL MODEL

μ_1 \ μ_2	0.04	0.05	0.06
0.04	1	0.036	0.262
0.05	0.944	1	0.121
0.06	0.832	0.141	1

From Figs. 5 and 6, the tendency of spiking activity has been to improve the anti-phase synchronization accuracy with decreasing of the coupling weight. Whereas, it has been to improve of in-phase synchronization accuracy with increasing of the coupling weight. Since the coupled Rulkov maps show high membrane potential and divergence by the increasing of absolute value of the coupling weight. From the result of Table 1, the P-P unidirectional model shows high accuracy in-phase/anti-phase synchronization by magnitude relation of the parameter μ.

Figure 7 shows the spiking activity and the coupling weight of P-I unidirectional model. We can see that the coupling weight close in the value to 0 from around $2500[ms]$, thus the coupled Rulkov maps show asynchronous firing. From this result, the intercalated cells provoke the asynchronous firing and convergence of the coupling weight in the unidirectional model.

C. 2 Coupled Maps of bidirectional model

In this section, we consider 2 coupled Rulkov maps of bidirectional models as shown in Fig. 8, and explain the synchronous firing phenomena compared to the 2 coupled Rulkov maps of unidirectional models.

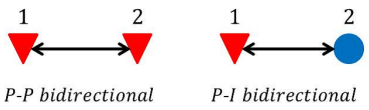

Fig. 8. Connective arrangements of 2 coupled maps in bidirectional model.

The spiking activity and the coupling weight of P-P bidirectional model is shown in Figs. 9, and Table 2 shows the synchronization probability of P-P bidirectional model if the parameter μ of coupled Rulkov maps is set to 0.04, 0.05 and 0.06.

From the results of Fig. 9 and Table 2, the coupled Rulkov maps of P-P bidirectional model shows in-phase synchronization. The P-P bidirectional model shows low accuracy in-phase/anti-phase synchronization compared to P-P unidirectional model, because the coupling weight closes in the value to 0.5 from beginning to end. Therefore, the P-P bidirectional model shows non-divergent spiking activity as shown in Fig. 8.

TABLE II
SYNCHRONIZATION PROBABILITY OF P-P BIDIRECTIONAL MODEL

μ_1 \ μ_2	0.04	0.05	0.06
0.04	1	0.726	0.474
0.05	0.806	1	0.849
0.06	0.848	0.18	1

Figure 10 shows the spiking activity and the coupling weight of P-I bidirectional model. From these results, the coupled Rulkov maps show asynchronous firing before $3000[ms]$, because the coupling weight close in the value to 0. However, the coupling weight close in the value to around -0.5 after $3500[ms]$, since the spiking activity shows high accuracy anti-phase synchronization and convergence of the coupling weight as shown in Fig. 10-(c).

From the results of 2 coupled Rulkov maps, the bidirectional models show the stable synchronous firing (i.e., non-divergence waveform) compared to unidirectional models. Moreover, the intercalated cells provoke the anti-phase synchronization firing and convergence of the coupling weight in the bidirectional model.

D. 3 Coupled Maps of unidirectional model

In this section, we consider 3 coupled Rulkov maps of unidirectional models as shown in Fig. 11. Figure 12 shows the spiking activity of P-P-P unidirectional model.

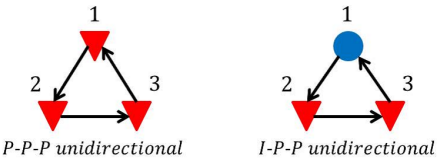

Fig. 11. Connective arrangements of 3 coupled maps in unidirectional model.

From the results of Fig. 12, the coupled Rulkov maps of P-P-P unidirectional model shows in-phase synchronization from beginning to end, and the tendency of spiking activity has been to improve the in-phase synchronization accuracy with time. Because this model is constructed by 3 pyramidal cells which is excitability neurons. In this simulation model, each pyramidal cells have a synergetic effect of increasing the coupling weights, thus the spiking activity shows divergent after $1400[ms]$ (i.e., lead to seizure).

Figure 13 shows the spiking activity of I-P-P unidirectional model. From Fig. 13-(b), the spiking activity of intercalated cell shows asynchronous firing with other pyramidal cells. However it obtains involved in the synchronization of pyra-

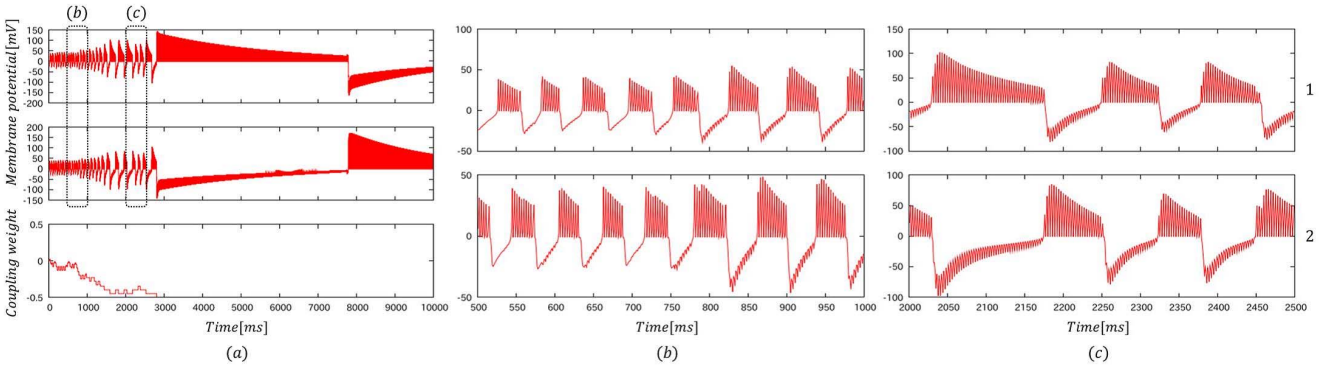

Fig. 5. Spiking activity and coupling weight of P-P unidirectional model (μ_1=0.04, μ_2=0.05). (a) 0$[ms]$-10000$[ms]$. (b) 500$[ms]$-1000$[ms]$. (c) 2000$[ms]$-2500$[ms]$.

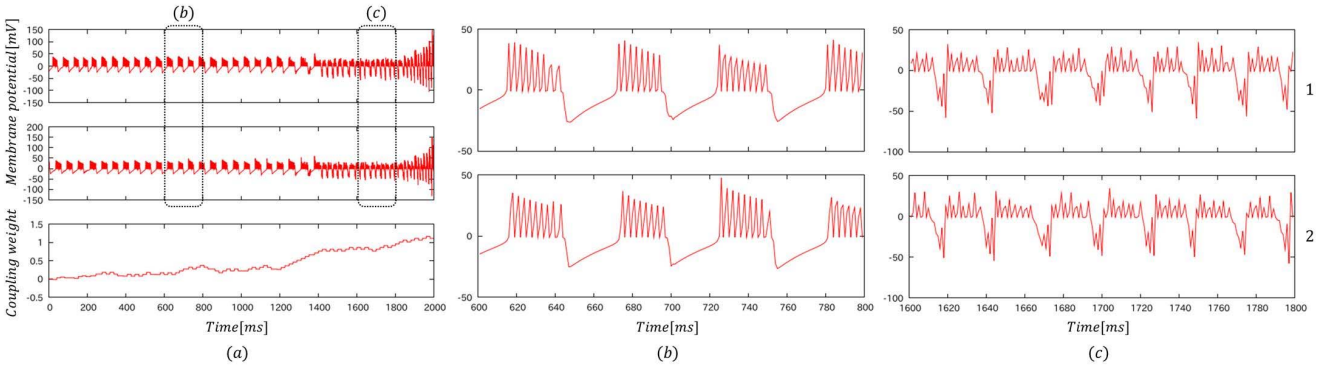

Fig. 6. Spiking activity and coupling weight of P-P unidirectional model (μ_1=0.05, μ_2=0.04). (a) 0$[ms]$-2000$[ms]$. (b) 600$[ms]$-800$[ms]$. (c) 1600$[ms]$-1800$[ms]$.

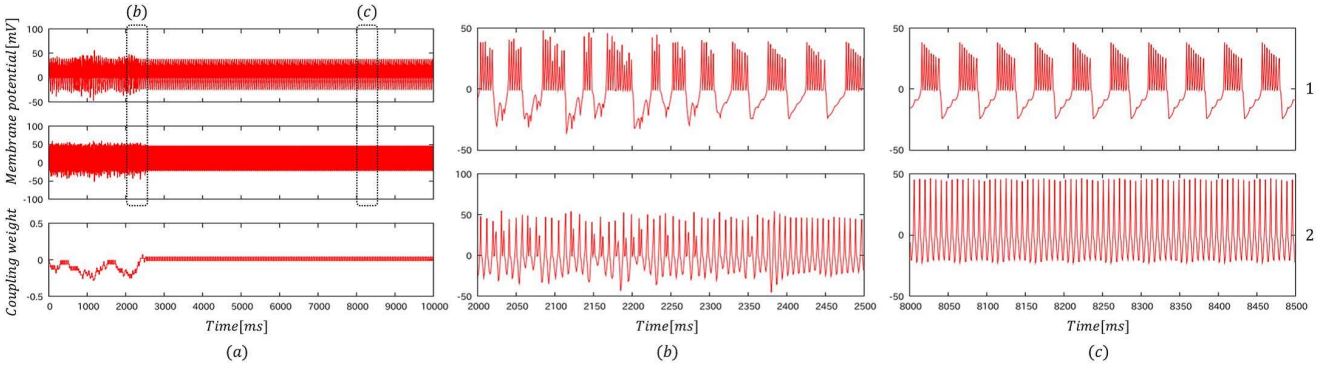

Fig. 7. Spiking activity and coupling weight of P-I unidirectional model. (a) 0$[ms]$-10000$[ms]$. (b) 2000$[ms]$-2500$[ms]$. (c) 8000$[ms]$-8500$[ms]$.

midal cells (From Fig. 13-(c)), since the spiking activity shows divergent after 1900$[ms]$ (i.e., lead to seizure).

E. 3 Coupled Maps of bidirectional model

In this section, we consider 3 coupled Rulkov maps of bidirectional models as shown in Fig. 14. Figure 15 shows the spiking activity of P-P-P bidirectional model.

From the results of Fig. 15-(b), the spiking activity of neuron 1 and 2 show the anti-phase synchronization, but neuron 3 shows asynchronous firing with other neurons. Since the neuron 3 obtains involved in synchronization of neuron 1 and 2, as shown in Fig. 15-(c). In this simulation

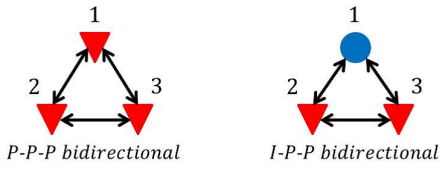

Fig. 14. Connective arrangements of 3 coupled maps in bidirectional model.

model, each pyramidal cells have a synergetic effect of increasing the coupling weights, thus the spiking activity shows divergent after 3300$[ms]$ (i.e., lead to seizure).

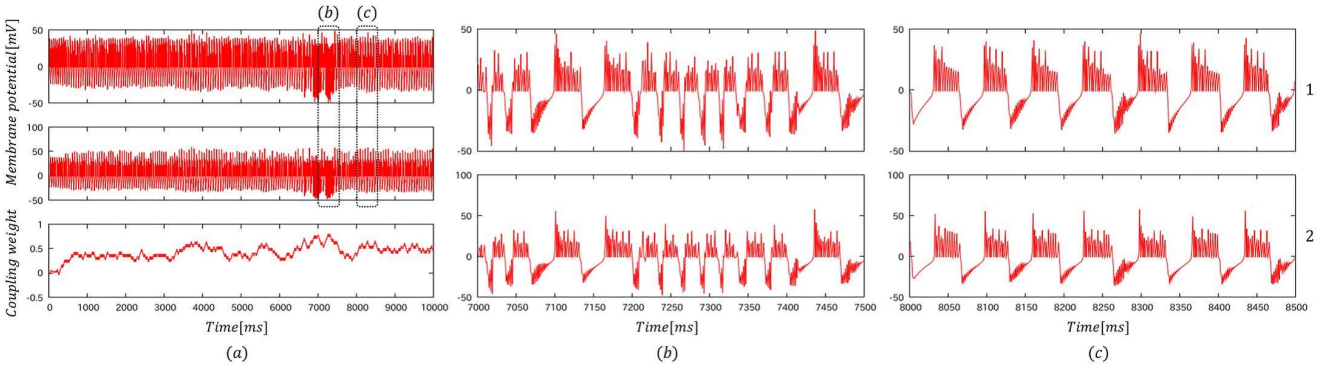

Fig. 9. Spiking activity and coupling weight of P-P bidirectional model. (a) $0[ms]$-$10000[ms]$. (b) $7000[ms]$-$7500[ms]$. (c) $8000[ms]$-$8500[ms]$.

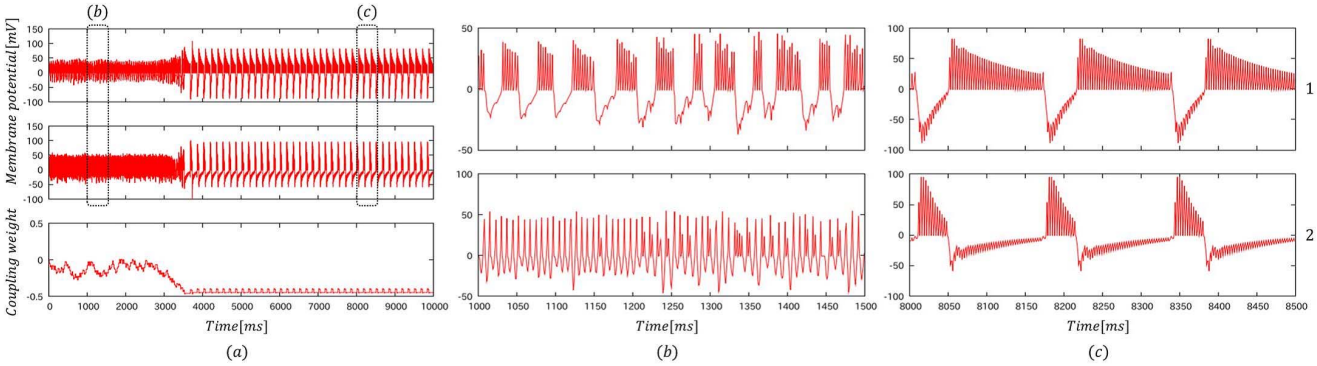

Fig. 10. Spiking activity and coupling weight of P-I bidirectional model. (a) $0[ms]$-$10000[ms]$. (b) $1000[ms]$-$1500[ms]$. (c) $8000[ms]$-$8500[ms]$.

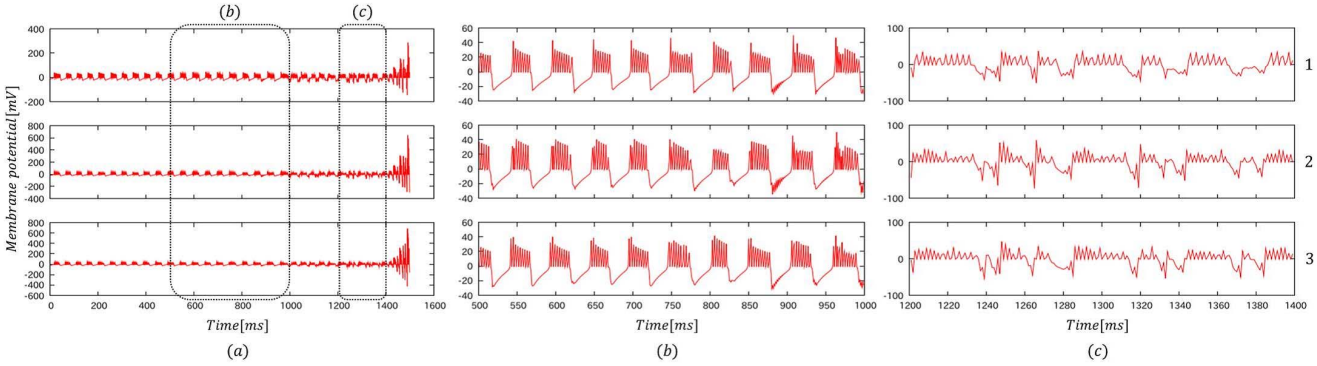

Fig. 12. Spiking activity of P-P-P unidirectional model. (a) $0[ms]$-$1500[ms]$. (b) $500[ms]$-$1000[ms]$. (c) $1200[ms]$-$1400[ms]$.

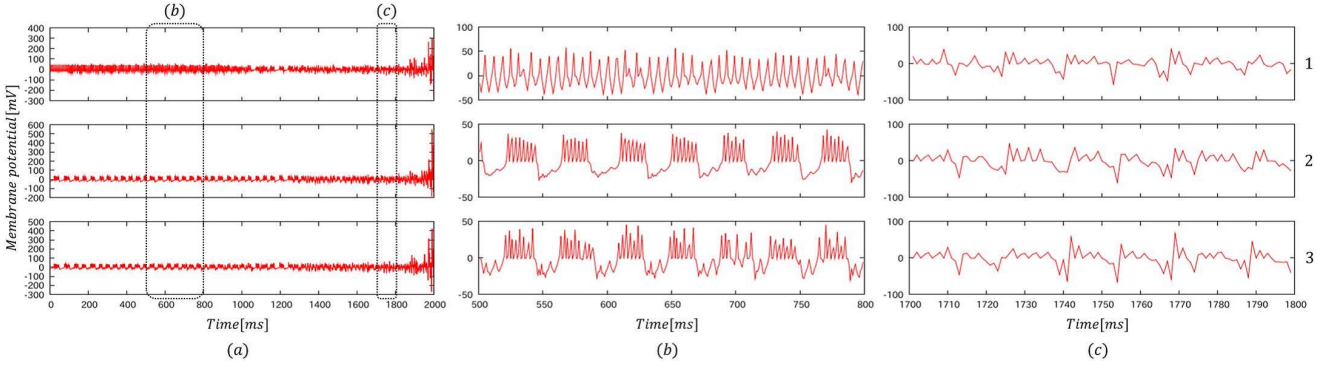

Fig. 13. Spiking activity of I-P-P unidirectional model. (a) $0[ms]$-$2000[ms]$. (b) $500[ms]$-$800[ms]$. (c) $1700[ms]$-$1800[ms]$.

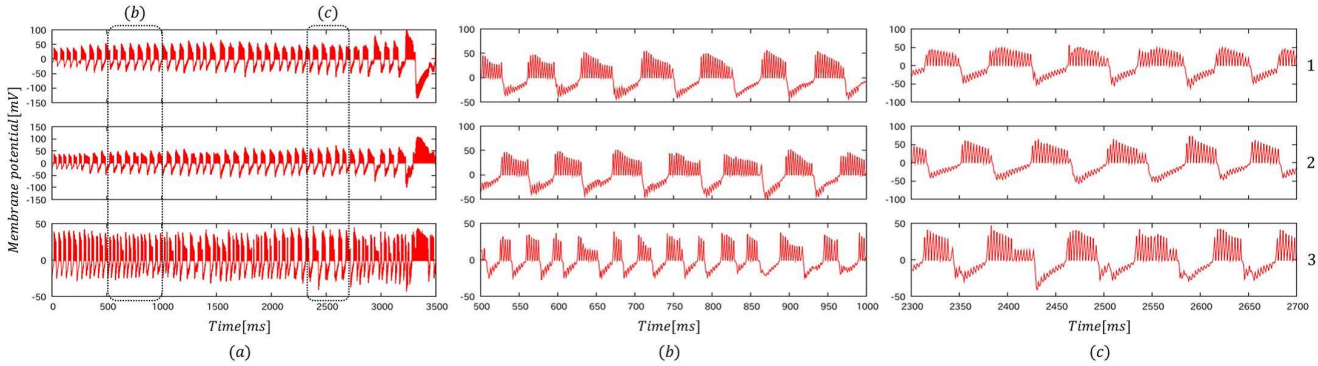

Fig. 15. Spiking activity of P-P-P bidirectional model. (a) $0[ms]$-$3500[ms]$. (b) $500[ms]$-$1000[ms]$. (c) $2300[ms]$-$2700[ms]$.

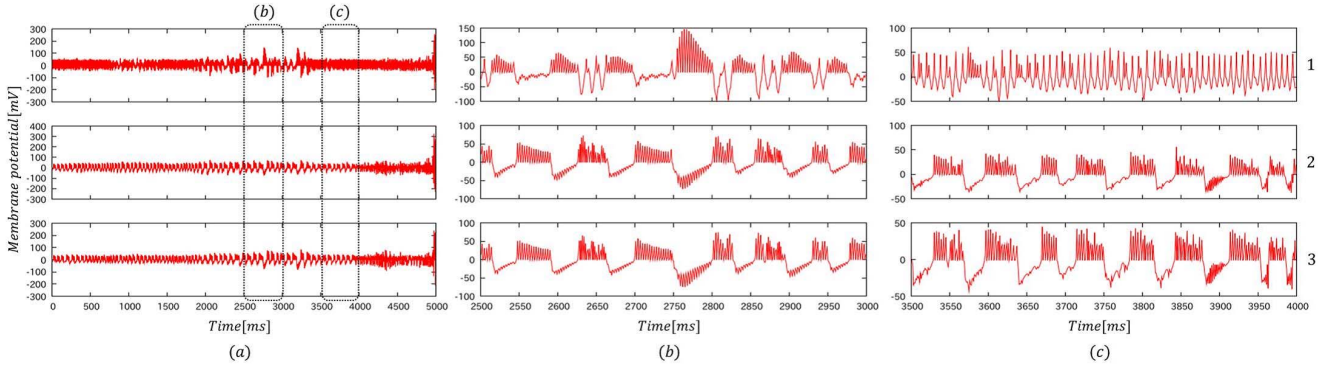

Fig. 16. Spiking activity of I-P-P bidirectional model. (a) $0[ms]$-$5000[ms]$. (b) $2500[ms]$-$3000[ms]$. (c) $3500[ms]$-$4000[ms]$.

Figure 16 shows the spiking activity of I-P-P bidirectional model. From Fig. 16-(b), the spiking activity of each neurons show high accuracy in-phase/anti-phase synchronization, since the neuron 1 (intercalated cell) gets out from in-phase synchronization of neuron 2 and 3 (From Fig. 16-(c)). However, the spiking activity shows divergent after $4900[ms]$ (i.e., lead to seizure), because each pyramidal cells (neuron 2 and 3) have a synergetic effect of increasing the coupling weights.

V. Conclusions

In this paper, we considered the simulation model which is constructed by using Rulkov maps with STDP. We investigated a relationship between synchronous firing and LTP, LTD. Moreover, we have explored the effect of unidirectional and bidirectional connection on spiking activity. From the simulation results, the coupled Rulkov maps show anti-phase synchronization, if STDP provokes the LTP of the synapses. Whereas, the coupled Rulkov maps show in-phase synchronization, if STDP provokes the LTD of the synapses. Additionally, the unidirectional models show high accuracy in-phase/anti-phase synchronization, and it shows divergent relatively early. The bidirectional models show the stable waveform (i.e., non-divergent) for a long term compared to unidirectional models.

References

[1] P. A. Schwartzkroin, "Role of the hippocampus in epilepsy," *Hippocampus*, vol. 4, pp. 239-242, 1994.

[2] K. Nakashima, H. Hayashi, O. Shimizu and S. Ishizuka, "Long-term change in synaptic transmission in CA3 circuits followed by spontaneous rhythmic activity in rat hippocampal slices," *Neuroscience Research*, vol. 40, pp. 325-336, 2001.

[3] A. Morrison, M. Diesmann and W. Gerstner, "Phenomenological models of synaptic plasticity based on spike timing," *Biological Cybernetics*, vol. 98, pp. 459-478, 2008.

[4] J. P. Pfister, W. Gerstner, "Triplets of spikes in a model of spike timing-dependent plasticity," *Journal of Neuroscience*, vol. 26, pp. 9673-9682, 2006.

[5] N. F. Rulkov, I. Timofeev and M. Bazhenov, "Oscillations in Large-Scale Cortical Networks: Map-Based Model," *Journal of Computational Neuroscience*, vol. 17, pp. 203-223, 2004.

[6] A. L. Shilnikov, N. F. Rulkov, "Origin of chaos in a Two-dimensional Map Modeling Spiking-Bursting Neural Activity," *Int. J. Bifurcation and Chaos*, vol. 13, pp. 3325-3340, 2003.

[7] N.F. Rulkov, "Modeling of Spiking-Bursting Neural Behavior using Two-dimensional Map," *Physical Review E*, vol. 65, 041922, 2002.

[8] D. Cumin, C. P. Unsworth, "Generalising the Kuromoto Model for the study of Neuronal Synchronisation in the Brain," *Phycsica D: Nonlinear Phenomena*, vol. 226, pp. 181-196, 2007.

[9] Yoshida M, Hayashi H, "Regulation of spontaneous rhythmic activity and organization of pacemakers as memory traces by STDP in the hippocampal CA3 model," *Phys. Rev. E*, 69 011910:1-15, 2004.